Int. J. Electrochem. Sci., 14 **(2019)** 7507 – 7515, doi: 10.20964/2019.08.35

International Journal of
ELECTROCHEMICAL
SCIENCE
www.electrochemsci.org

Short Communication

N-doped MoS_2 Nano-Flowers as High-Performance Anode Electrode for Excellent Lithium Storage

Shuhua Li[1,2,*], *Dawei Qu*[1], *Peng Wang*[2], *Yongjia Wang*[2], *Fei Xie*[2]

[1] State Key Laboratory of Automotive Simulation and Control, Jilin University, Changchun 130025, China
[2] Department of Vehicle Engineering, Hefei University of Technology, Hefei 230009, China
[*]E-mail: shuhualijl@sohu.com

Received: 15 March 2019 / *Accepted:* 14 May 2019 / *Published:* 30 June 2019

N-doped MoS_2 nano-flowers are successfully synthesized and used as the anode materials for the lithium-ion batteries. The electronic conductivity of the MoS_2 anode materials could be effectively improved by the nitrogen doping process. Compared with the pristine MoS_2 anode electrodes, the N-doped MoS_2 anode electrodes exhibit specific capacity value of 786 mAh g^{-1} after 100 cycles at the high current density of 0.5 C, demonstrating excellent cycle stability. This stable cycle performance is ascribed to the superior electronic conductivity of the N-doped MoS_2 anode, which could provide pathways for the transport of the electronics.

Keywords: MoS_2 anode; N-doped; Cycle stability; Specific capacity.

1. INTRODUCTION

Lithium–ion batteries are the main power sources for the electric vehicles and electronic equipment. The lithium-ion batteries are consisted of cathode, anode and electrolyte [1, 2]. Among these components, anode plays a key role for the electrochemical performance of the lithium-ion batteries. Therefore, many researchers are studying the employment of various anode materials. In the reported anode materials, metal sulfide MoS_2 has high theoretical capacity, large density and stable chemical properties [3, 4]. As a result, the MoS_2 anode becomes the hot topic for the researchers all over the world. Whereas, the MoS_2 anode materials also have some disadvantages [5] .

As we all know, the MoS_2 suffers from poor electronic conductivity during the electrochemical process [6, 7]. Besides, volume expansion will take place when the lithium is intercalated into the MoS_2 layer. Many works have been reported about modifying the electrochemical performance of the MoS_2 anode [8, 9]. Huang et al have prepared MoS_2 hierarchical microspheres as anode material for

lithium-ion batteries [10]. The as-prepared MoS_2 microspheres kept the capacity of 768 mAh g^{-1} after 50 cycles at 0.1 C. It can be proved that perfect structure has positive effect on improving the electrochemical performance.

In this paper, N-doped MoS_2 nano-flowers are successfully synthesized and used as the anode materials for the lithium-ion batteries. The electronic conductivity of the MoS_2 anode materials could be effectively improved by the nitrogen doping process. Moreover, the unique structure of the MoS_2 materials could buffer the volume change during discharge and charge process. As a result, comparing with the pristine MoS_2 anode electrodes, the as-prepared N-doped MoS_2 anode electrodes exhibit specific capacity value of 786 mAh g^{-1} after 100 cycles at the high current density of 0.5 C, demonstrating excellent cycle stability.

2. EXPERIEMENTAL

2.1. Preparation of the N-doped MoS_2 nano-flowers

0.38 g ammonium heptamolybdate tetrahydrate and 1.2 g thiourea were dissolved in 50 mL deionized water and stirred for 30 min. Then, the mixture was transferred to a 80 mL teflon-lined autoclave and kept at 180 ºC for 24 h. When the reaction was finished, the products were collected by centrifugation and washing with water and ethanol for several times. After that the N-doped MoS_2 materials are prepared under NH_3 atmosphere at 300 ºC for 2 h. Finally, the pure MoS_2 and N-doped MoS_2 materials are separated into two kinds samples, respectively.

2.2. Materials characterization

The morphology of the as-obtained samples was characterized by using a scanning electron microscope (SEM, JSM-7001F). The structure of the materials was tested by X-ray diffractometer (XRD, D8 Advance, BRUKER). The porous structure was measured by using BET method. XPS was used to investigate the element valence in the samples.

2.3 Electrochemical measurements

The electrochemical performance was measured by using coin-type half batteries. A slurry was prepared by mixing 80 wt.% samples, 10 wt.% acetylene black and 10 wt.% PVDF with NMP. Then, the slurry was uniformly casted onto a Cu foil with a doctor blade to prepare a film-type electrode. The process of preparing batteries is conducted in the Ar-filled glove box. The lithium is used as the counter electrode. The electrolyte includes 1.0 M $LiPF_6$ and EC/DEC (1:1). All electrochemical measurements were carried out on a battery testing system (LAND CT 2001A) in the potential range from 0.01 V to 3 V.

3. RESULTS AND DISCUSSION

Figure 1 is the XRD pattern of N-doped MoS_2 and pure MoS_2 materials. The diffraction pattern of the pure MoS_2 indicates that the prepared MS has good crystallinity and no impurity peaks. The purity of the materials has direct effect on the performance of the lithium-ion batteries. As shown in Figure 1, the as-prepared MS samples display typical diffraction peaks of metal sulfide MoS_2, indicating the high purity of the MoS_2 samples. The peaks at 13°, 34°, 56° are corresponding to the (101), (111) and (110) crystal plane, respectively [11, 12]. For the N-MS samples, the diffractions have no obvious changes comparing with the pure MS samples. Therefore, it can be obtained from the XRD result that the N-MS and MS samples are prepared successfully.

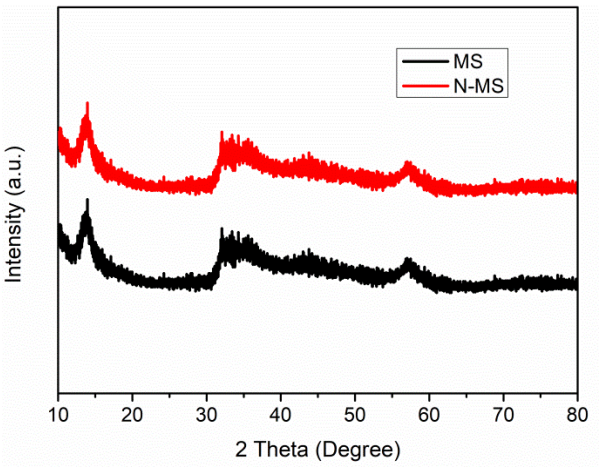

Figure 1. XRD patterns of the N-MS and MS.

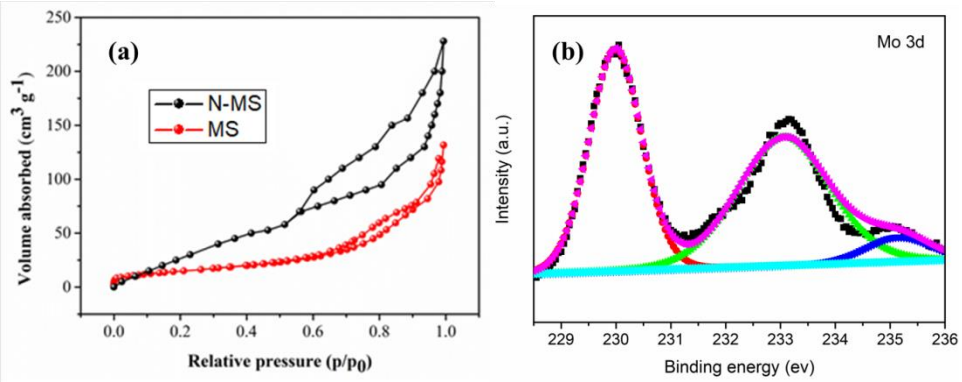

Figure 2. (a) Nitrogen sorption isotherms of the N-MS and MS. (b) The XPS spectra of Mo 3d for the N-MS.

Figure 2a shows the N_2 adsorption isotherms of N-MS and MS samples. It can be seen that the as-prepared MS sample shows no obvious porous structure. This character has negative effect on the transport of the Li^+ [13, 14]. However, after N-doping process for the MS sample, the N-MS

composites shows typical mesoporous structure, which could provide channels for the transport of Li^+ in the electrolyte [15, 16, 17]. To further study the element valence in the as-prepared samples, XPS test was conducted for the N-MS. As shown in Figure 2b, the spectra of Mo 3d shows peaks at 230.3 eV and 233.1 eV, respectively [18]. These two peaks are corresponding to the Mo-Mo chemical bond and Mo-S bond, respectively.

Figure 3a is the SEM image of the MS sample. The MS sample shows nano-flower morphology. Besides, it can be clearly seen that the surface of the MS nano-flower is constructed by many nano-sheets. The dimeter of the MS nano-flower is located at 120 nm. Figure 3b shows the morphology of the N-MS composites. The N-MS exhibits similar morphologies comparing with the pure MS samples. All of the N-MS nano-flowers are uniformly dispersed in the image. In all, comparing with the pure MS samples, the overall morphology of N-MS composite is much better, and the electronic conductivity can be improved via the N-doping during the electrochemical process. To confirm the presence of all elements in the N-MS composites, EDS was conducted for the N-MS composites. As shown in Figure 3c-f, it can be clearly observed that the elements Mo, S and N are distributed in the N-MS composites. This also could prove that the N-doped MoS_2 composites are successfully prepared.

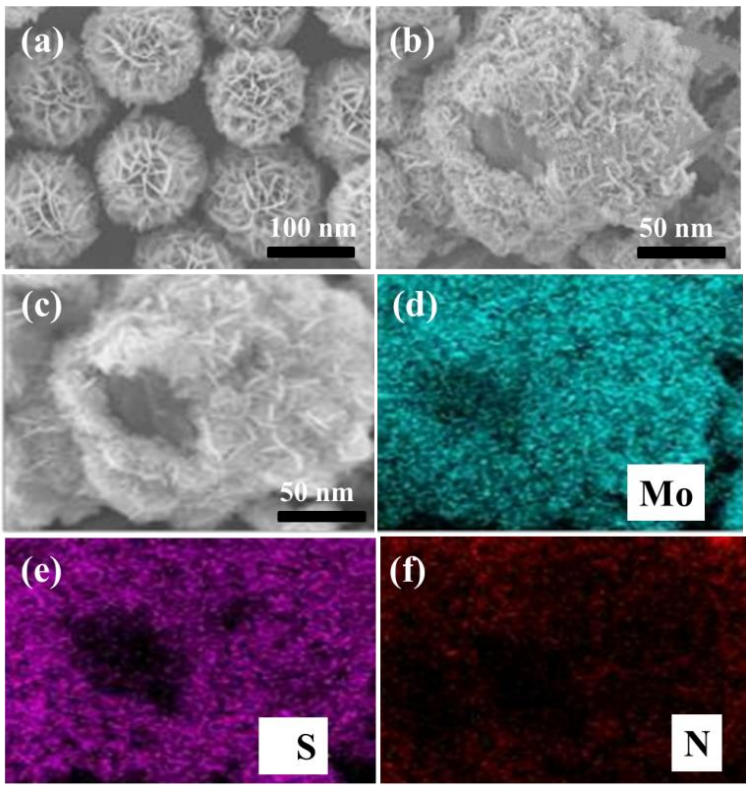

Figure 3. SEM images of (a) MS, (b) N-MS. (c), (d), (e), (f) SEM image of N-MS and corresponding elements mapping of Mo, S and N.

The constant discharge/charge profiles of the electrodes are tested between 0-3 V at the current density of 0.1 C. As shown in Figure 4a, the initial specific capacity of the N-MS anode electrode is 1186 mAh g^{-1}. For the pure MS anode electrode, the initial specific capacity value is only about 986 mAh g^{-1} at the current density of 0.1 C. This is due to the improved electronic conductivity of the as-prepared N-MS anode electrode, which is improved by N-doping process. Figure 4b shows the discharge/charge profiles of the electrodes after 10 cycles. It can be seen that the voltage platform at 0.9 V is disappeared, which is ascribed to the irreversible phase transition during the discharge/charge process.

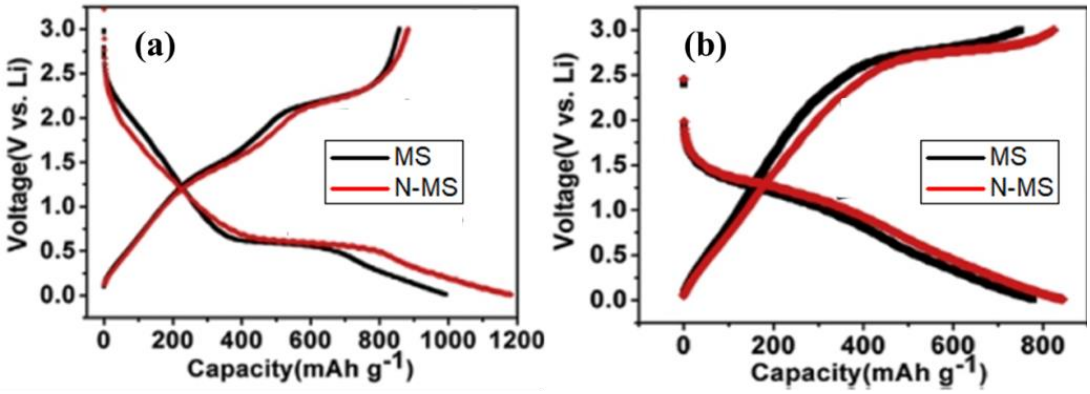

Figure 4. (a) The 1st and (b) 10th constant discharge/charge profiles of the MS and N-MS electrode.

Figure 5a compares the cycle performance of MS and N-MS composites. The specific capacity of the N-MS composites can remain at 738 mAh g^{-1} at the current density of 0.5 C after 100 electrochemical cycles. However, the specific capacity of the pure MS anode electrode is 629 mAh g^{-1}. This is because the pure MS anode electrodes suffer from poor electronic conductivity during the electrochemical cycles. Besides, the structure of the pure MS anode electrodes may be damaged by the high current density [22, 23]. For the N-MS anode, the proicess of the N-doping can effectively enhance the conductivity and inhibit the volume change.

Figure 5b shows the rate performance of the pure MS anode electrode and N-MS anode at various current densities form 0.1 C to 2 C. The as-prepared N-MS anode displays excellent rate performance Even when the discharge/charge process is after the 25 cycles, the specific capacity remains at 495 mAh g^{-1} at the high current density of 2 C. Moreover, when the current density returns to 0.1 C, the capacity of the N-MS anode could recover at 883.2 mAh g^{-1}, which is far higher than the pure MS anode electrode. However, the pure MS anode electrode shows bad rate performance during the change of the current densities. Therefore, it could be proved that the N-MS anode electrode has better rate performance and good reversibility than pure MS anode.

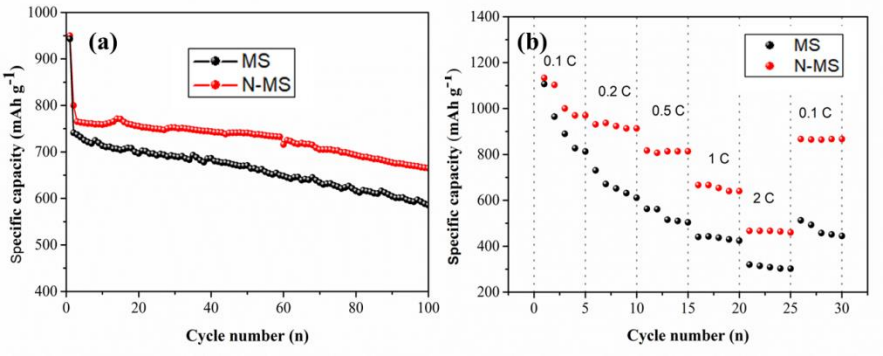

Figure 5. (a) The cycle performance of the N-MS and MS anode at the current density of 0.5 C. (b) The rate performance of the N-MS and MS anode at the current densities from 0.1 C to 2 C.

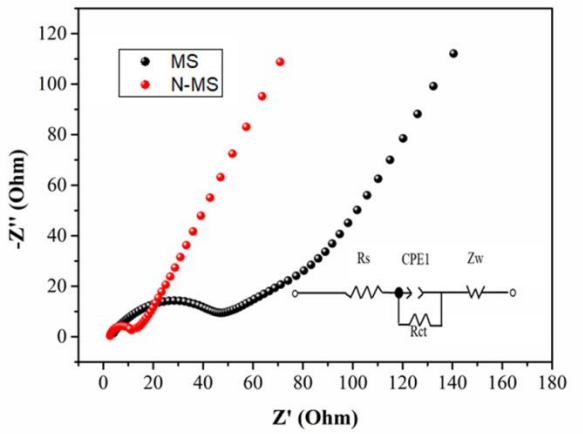

Figure 6. Electrochemical impedance spectra of the N-MS and MS anode electrode.

In order to further confirm the superior conductivity of the N-MS anode electrode, EIS test was conducted. As shown in Figure 6, there are semicircle and slant line in the spectra. The semicircle in the high frequency represent charge transfer impedance (Rct) on the electrode surface. The slant line in the and low frequency regions is corresponding to the diffusion impedance (Rs) of Li^+. From the spectra, it can be seen that the N-MS has smaller charge transfer impedance and Warburg impedance [19, 20]. Consequently, the perfect electrochemical performance can be attributed to the N-doping process, which could effectively enhance the electronic conductivity of the pure MS anode electrode. Moreover, it provides pathway for the transport of Li^+ between the electrolyte and electrode [21]. Therefore, it can be concluded that the as-prepared N-MS composites has superior electronic conductivity, which could improve the electrochemical performance of the lithium-ion batteries.

Furthermore, table 1 shows the values of Rs and Rct value for the N-MS and MS anode electrodes, respectively. Form the table, it can be seen that the Rs and Rct for N-MS anode is 5.32 Ω and 12.65 Ω, respectively. This value is much smaller than pure MS anode, demonstrating superior electronic conductivity. This impedance value further clearly confirms the superior electronic conductivity of the N-MS anode materials by N-doping process.

Table 1. Kinetic parameters obtained from fitting EIS for the N-MS and MS anode electrodes.

Electrodes	Rs (Ω)	Rct (Ω)
MS	6.85	50.68
N-MS	5.32	12.65

Table 2 shows the electrochemical performance of the various anode materials for the lithium-ion batteries. As shown in Table 2, it can be clearly seen that the as-prepared N-MS anode electrode exhibits more excellent cycle stability than other reported anode materials in the references. As for the reason, it may be ascribed to the improved electronic conductivity of the N-MS anode, which is N-doped. Moreover, the unique structure of the MoS_2 materials could buffer the volume change during discharge and charge process. In all, our work may provide a new strategy to enhance the electrochemical performance of the MoS_2-based anode by modifying the electronic conductivity.

Table 2. Comparison of the N-MS anode materials with other similar anode materials for the lithium-ion batteries.

Electrode	Current	Capacity (mAh g^{-1})	Ref
TiO_2@MoS_2	0.1 C	597 (100 cycles)	24
MoS_2/G	0.1 C	660 (50 cycles)	25
MoS_2/XC-72	0.1 C	610 (100 cycles)	26
N-MS	0.5 C	738 (100 cycles)	This Work

4. CONCLUSIONS

N-doped MoS_2 nano-flowers are successfully synthesized and used as the anode materials for the lithium-ion batteries. The electronic conductivity of the MoS_2 anode materials could be effectively improved by the nitrogen doping process. Moreover, the unique structure of the MoS_2 materials could buffer the volume change during discharge and charge process. Compared with the pristine MoS_2 anode electrodes, the N-doped MoS_2 anode electrodes exhibit specific capacity value of 786 mAh g^{-1} after 100 cycles at the current density of 0.5 C, demonstrating excellent cycle stability. This stable cycle performance is ascribed to the superior electronic conductivity of the N-doped MoS_2 anode, which could provide pathways for the transport of the electronics.

ACKNOWLEDGEMENTS
This work was supported by the Foundation of State Key Laboratory of Automotive Simulation and Control (20171111) and the National Key Research and Development Program of China (2016YFB0100300).

References

1. Y. G. Huang, Y. Wang, X. H. Zhang, F. Y. Lai, Y. N. Sun, Q. Y. Li and H. Q. Wang, *Mater*. Lett., 243 (2019) 84.
2. Y. X. Zhang, J. Shao, Y. K. Tao S. R. Wang, *J. Alloy Compd*., 737 (2018) 477.
3. M. Q. Zhang, X. Bai, Y. Y. Liu, Y. P. Zhang, Y. Wu, D. L. Cui, Y. Liu, L. Wang, B. Li and X. T. Tao, *Appl. Surf. Sci.*, 469 (2019) 923.
4. Y. Li, C. Li, H. Qi, K. F. Yu and C. Liang, *Chem. Phys*., 506 (2018) 10.
5. D. P. Aurelien, I. Plitz, S. Menocal and G. Amatucci, *J. Power Sources*, 115 (2003) 171.
6. K. Y. Qi, Z. M. Yuan, Y. Hou, R. C. Zhao and B. W. Zhang, *Appl. Surf. Sci.*, 483 (2019) 688.
7. C. R. Li, H. Song, C. M. Mao, H. R. Peng and G. C. Li, *J. Alloy Compd.*, 786 (2019) 169.
8. N. Q. Hai, S. H. Kwon, H. Kim, T. Kim, S. G. Lee and J. H. Hur, *Electrochim. Acta*, 260 (2018) 129.
9. Y. Y. Chen, Y. Wang, H. X. Yang, H. Gan, X. W. Cai, X. M. Guo, B. Xu, M. F. Lv and A. H. Yuan, *Cream. Int*., 43 (2017) 9945.
10. M. Zheng, R. S. Guo, Z. C. Liu, B. Y. Wang, L. C. Meng, F. Y. Li, T. T. Li and Y. N. Luo, *J. Alloy Compd*., 735 (2018) 1262.
11. Y. Wang, B. F. Wang, F. Xiao, Z. G. Hunag, Y. J. Wang, C. Richardson, Z. X. Chen, L . F. Jiao and H. T. Yuan, *J. Power Sources*, 298 (2015) 203.
12. O. K. Park, Y. H. Cho, S. H. Lee, H. C. Yoo, H. K. Song and J. Cho, *Energ. Environ. Sci.*, 4 (2011) 1621.
13. M. Hirayama, H. Ido, K. S. Kim, W. Cho, K. Tamura, J. Mizuki and R. Kanno, *J. Am. Chem. Soc*., 132 (2010) 15268.
14. A. Yamada, M. Tanaka, K. Tanaka and K. Sekai, *J. Power Sources*, 81 (1999) 73.
15. V. G. Kumar, J. S. Gnanaraj, S. B. David, D. M. Pickup, E. H. Eck and A. Gedanken, *Chem. Mater*., 15 (2003) 4211.
16. J. F. Wu, L. Zuo, Y. H. Song, Y. Q. Chen, R. H. Zhou, S. H. Chen and L Wang, *J. Alloy Compd*., 656 (2016) 745.
17. X. Zheng, Y. H. Zheng, H. J. Zhang, Q. L. Yang and C. X. Xiong, *Chem. Eng. J*., 370 (2019) 547.
18. B. Li, X. G. Wei, Z. R. Chang, X. N. Chen, X. Z. Yuan and H. J. Wang, *Mater. Lett*., 135 (2014) 75.
19. Y. L. Ding, J. A. Xie, G. S. Cao, T. J. Zhu, H. M. Yu and X. B. Zhao, *Adv. Funct. Mater.*, 21 (2011) 348.
20. W. Tang, X. J. Wang, Y. Y. Hou, L. L. Li, H. Sun, Y. S. Zhu, Y. Bai, Y. P. Wu, K. Zhu and T. Ree, *J. Power Sources*, 198 (2012) 308.
21. D. K. Kim, P. Muralidharan, H. W. Lee, R. Ruffo, Y. Yang, C. K. Chan, H. L. Peng, R. A. Huggins and Y. Cui, *Nano lett*., 8 (2008) 3948.
22. Y. G. Huang, C. Ji, Q. C. Pan, X. H. Zhang, J. J. Zhang, H. Q. Wang, T. Liao and Q. Y. Li, *J. All. Compd*, 728 (2017) 1139.
23. Z. J. Wang, M. Liu, G. J. Wei, P. Han, X. X. Zhao, J. X. Liu, Y. Zhou and J. Zhang, *Appl. Surf. Sci*., 423 (2017) 375.
24. D. M. Qi, S. Li, Y. H. Chen and J. G. Huang, *J. Alloy Compd*., 728 (2017) 506.
25. Q. H. Liu, Z. J. Wu, Z. L. Ma, S. Dou, J. H. Wu, L. Tao, X. Wang, C. B. Quyang, A. L. Shen and S. Y. Wang, *Electrochim. Acta*, 177 (2015) 298.

26. X. F. Zhou, Z. Wang, W. X. Chen, L. Ma, D. Y. Chen and J. Y. Lee, *J. Power Sources*, 251 (2014) 264.